

## STUDY ON DAMPING PROPERTY AND VIBRATION BEHAVIOUR OF SDOF SYSTEM

Manoj Acharya<sup>1\*</sup>, Sailesh Mishra<sup>1</sup>, Bishwojit Singh<sup>1</sup>, Reetu Adhikari<sup>1</sup>, Nihit Koirala<sup>1</sup>, Mahesh Raj Bhatt<sup>1</sup>

<sup>1</sup> Department of Civil Engineering, Kathmandu University, Nepal

---

### Abstract

The damping ratio is a critical parameter in vibration analysis, representing the energy dissipation capacity of structural components. Accurate assessment of damping behaviour is essential for predicting the dynamic response of structures such as machinery, buildings, and bridges. This study aims to determine the damping ratio of a SDOF system using the logarithmic decrement method. Physical SDOF system were fabricated from mild steel sections measuring 20 mm in width and 3 mm in thickness, with a 1 kg lumped mass attached at the free end to simulate dynamic loading. Free vibration tests were conducted, and displacement-time data were measured using a VLX50LOX sensor. The damping ratio were calculated by applying the logarithmic decrement formula to the decay of successive vibration amplitudes. Initially numerical computation was conducted by setting the time periods between 0.5 and 1.5 seconds by varying length of SDOF system. The Rayleigh method, Finite Element Method (FEM) and the lumped mass concept were used to calculate corresponding SDOF system length. Means of the sum of lengths calculated at each time period were applied to the analysis of SDOF system using ETABS application software. The preparation of physical specimens was based on these numerical findings, and free vibration experiments were carried out on fabricated specimens. The displacement vs time was measured by a VLX50LOX sensor, and then damping ratio with logarithmic decrement method was determined. The damping ratios obtained for the SDOF specimens were from 0.0042 to 0.0055. This setup can be used as an experimental apparatus for studying a single-degree-of-freedom (SDOF) system in the laboratory.

**Keywords:** Damping ratio; Cantilever beam; Logarithmic decrement; Free vibration; Lumped mass

---

### 1. Introduction

Vibration is the oscillatory motion of a structure or system about its equilibrium position due to dynamic forces. According to Chopra (2007), vibration is an essential aspect of structural dynamics, as understanding it allows engineers to predict the response of structures under dynamic loads such as wind, earthquakes, or machinery excitations. Uncontrolled vibrations can lead to fatigue, noise, discomfort, or even structural failure.

Damping is the property of a structure or material that dissipates vibrational energy, thereby reducing the amplitude of oscillations over time. As stated by Clough and Penzien (1975), damping arises due to mechanisms

such as internal material hysteresis, friction, or interaction with the surrounding medium, and it plays a critical role in controlling structural vibrations. Accurate knowledge of damping is necessary to predict dynamic response, prevent resonance, and ensure the safety and serviceability of engineering systems.

Cantilever beams are widely used structural elements in engineering applications, including building overhangs, bridges, and machinery supports. Their dynamic behaviour, including natural frequencies, mode shapes, and damping characteristics, must be understood to design safe and reliable structures (Chopra, 2007). Among experimental techniques, the logarithmic decrement method provides a practical way to determine the damping coefficient by analysing the decay of free vibrations (Clough & Penzien, 1975)

Mevada and Patel (2016) investigated the structural damping effect on cantilever beam vibrations made of

---

\*Corresponding author: Manoj Acharya  
Department of Civil Engineering, Kathmandu University, Nepal  
Email: aacharyamanoj51@gmail.com  
<https://doi.org/10.3126/jscce.v13i1.89608>

aluminum, brass, and steel using impact hammer tests and LabVIEW. They estimated the natural frequency and damping ratio experimentally and validated results through harmonic analysis in ANSYS using the Half-Power Bandwidth Method. Their results showed that brass exhibited the highest damping ratio, followed by steel and aluminium, highlighting the influence of material properties on vibration behavior.

Brahmam (2022) conducted experimental studies on damping estimation in cantilever beams using various techniques such as Logarithmic Decrement, Circle Fit, Half-Power Bandwidth, F-D Curve, and Sine Sweep methods. The study implemented MATLAB-based data analysis to compare damping ratios obtained from each method, concluding that results vary with excitation and response conditions, highlighting the influence of frequency range and sweep rate on damping accuracy.

Desai (2021) performed experimental determination of damping factors for steel plates with and without rubber coating using Fast Fourier Transform (FFT) and Dewesoft software under forced vibration conditions. The study found that rubber coating significantly increased the damping factor, reducing the vibration amplitude, with experimental damping values closely matching standard references. The author highlighted the importance of accurate damping estimation for improving vibration control and structural performance.

The study is intended to determine the damping ratio of a SDOF system using the logarithmic decrement method by analyzing its free vibration response, recording successive amplitude peaks, and calculating the damping ratio from the exponential decay of vibration amplitudes. This research involves conducting free vibration experiments on SDOF specimen to record its oscillation decay over time. The experimental data will be processed to calculate the logarithmic decrement and corresponding damping ratio.

## 2. Methodology

The present study aims to determine the damping ratio ( $\xi$ ) of a SDOF system using the logarithmic decrement method based on experimentally recorded free vibration data. The complete methodology involves analytical estimation, numerical validation, experimental measurement, and data analysis using MATLAB.

### 2.1. Selection of Material and SDOF System Dimensions

A SDOF system with a rectangular cross-section of 3 mm × 20 mm was selected for the study due to its elastic behaviour and availability. The SDOF system was designed to carry a lumped mass of 1 kg at its free end to simulate practical loading conditions and to control the vibration characteristics.

### 2.2. Determination of SDOF System Length for Target Time Periods

To analyse the influence of time period on damping behaviour, four target natural time periods were chosen: 0.5 s, 0.75 s, 1 s, and 1.25 s. For each target time period, the required length of the SDOF system was calculated using three different analytical approaches:

#### 2.2.1 Lumped mass concept

The system was idealized as a single-degree-of-freedom (SDOF) and the natural Time was determined using classical vibration theory as shown in equation 1.

$$T = 2\pi\sqrt{\frac{K}{M}} \quad (1)$$

#### 2.2.2 Rayleigh's method

The SDOF system distributed mass and deformation shape were considered to estimate the fundamental time period based on strain and kinetic energy relations.

#### 2.2.3 Finite Element Method (FEM)

The beam was discretized into finite elements to obtain its natural frequency numerically, assuming Euler–Bernoulli beam behaviour.

#### 2.2.4 Numerical verification using ETABS

To verify the analytical calculations, the SDOF system with lumped mass was modelled in ETABS. A linear modal analysis was performed to determine the fundamental time period of vibration. The obtained numerical results were compared with the targeted time periods (0.5–1.25 s), and the differences were found to be within a minimal tolerance, validating the accuracy of the analytical length estimation.

#### 2.2.5 Determination of permissible displacement

Before conducting the physical experiment, the maximum permissible tip displacement of the SDOF system was calculated to ensure that bending stresses remained within the elastic limit. The allowable displacement was computed using the bending stress concept as in Equation 2 and 3, ensuring that the b SDOF system did not enter the plastic region during free vibration

$$\frac{M}{I} = \frac{\sigma}{y} = \frac{E}{R} \quad (2)$$

$$\Delta = \frac{2 \times \sigma a l \times L^2}{3ED} \quad (3)$$

**Where:**

- $\sigma$ : bending stress of the material
- $L$ : length of the SDOF system
- $E$ : Young’s modulus of elasticity.
- $D$ : depth (thickness) of the plate section

The formula ensures bending stress at the fixed end does not exceed the allowable limit.

*Derived from combining the bending stress equation and deflection formula for a cantilever with tip load.*

**2.2.6 Experimental setup and data acquisition**

The physical SDOF system was fabricated based on the validated dimensions. The free vibration test was performed by deflecting the SDOF system up to the permissible displacement and releasing it suddenly to allow free oscillation. The experimental setup illustrating the physical arrangement of the four SDOF system is presented in Figure 1.



Figure 1: Experimental setup showing physical arrangement of the four SDOF System Prepared in Kathmandu University Structural Engineering Laboratory

A Time-of-Flight (ToF) light-reflecting sensor was used to accurately measure the displacement-time response of the SDOF system tip during vibration. The sensor output was recorded as displacement versus time data for subsequent analysis. The experimental setup of the VLX50LOX Time-of-Flight (ToF) sensor interfaced with Arduino is illustrated in Figure 2.

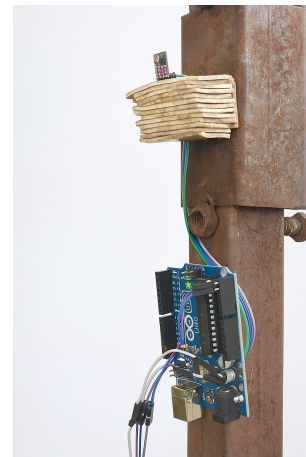


Figure 2: Arduino-based time-of-flight sensor setup for distance measurement

**2.2.7 Damping ratio determination**

The recorded displacement time data were processed in MATLAB to extract the logarithmic decrement ( $\delta$ ) from successive peak amplitudes using the relation as shown in the Equation 4.

$$\xi = \frac{1}{2\pi n} \times \ln \left( \frac{X_1}{X_{n+1}} \right) \quad (4)$$

Where  $x_1$  and  $x_{n+1}$  are the amplitudes of the first and (n+1)th cycles, respectively.

The damping ratio, denoted as  $\xi$ , was determined from the free vibration response of each recorded through the Time-of-Flight (ToF) light reflection sensor. The displacement–time data were imported into MATLAB for post-processing and analysis.

As the damping ratio primarily depends on the rate of reduction in the vibration amplitude over successive cycles, the determination was carried out by analysing the peak amplitudes of the response curve. The procedure followed is as described below:

1. The upper peaks (positive amplitudes) of the displacement–time response were first identified.
2. The damping ratio  $\xi$ , was calculated using the logarithmic decrement method, considering the amplitude reduction between the first and second peaks.
3. The process was repeated by taking the first and third peaks, then the first and fourth peaks, and so on. This provided a series of damping ratio values corresponding to each upper peak pair.

4. Similarly, the lower peaks (negative amplitudes) were extracted from the response data, and corresponding values of  $\xi$ , were determined using the same approach..
5. The average damping ratio from upper peaks and the average damping ratio from lower peaks were each computed separately.
6. Finally, the overall average damping ratio for the data set was obtained by averaging these two mean values.

### 3. Result and Discussion

This work focuses on evaluating the damping ratio of a steel SDOF system with a 3 mm × 20 mm cross-section. Four SDOF system configurations were considered to achieve target natural time periods of 0.5 s, 0.75 s, 1.0 s, and 1.25 s, each equipped with a 1 kg mass at the free end. Analytical calculations were performed using MATLAB, and the resulting natural time periods were verified through ETABS modelling.

#### 3.1. Determination of SDOF System Length for Target Periods

Initially, the required SDOF system lengths corresponding to each target time period were determined using three independent approaches:

1. Lumped Mass Concept
2. Rayleigh's Method
3. Finite Element Method (FEM)

The MATLAB analysis results for all three methods are presented in Table 1, which shows a close agreement among the computed lengths. This agreement confirms the validity and consistency of the theoretical approaches used.

We take length obtain from the FEM method for our analysis. The analytical computation and data processing were carried out using MATLAB.

#### 3.2. Verification Using ETABS Model

To validate the analytically obtained lengths, each SDOF system was modelled in ETABS with fixed-free boundary conditions and a 1 kg lumped mass at the free end. The modal analysis results indicated that the fundamental time periods from ETABS closely matched the target periods obtained from MATLAB analysis, with a deviation of less than 12 %. As shown in the Table 2. This consistency confirms that the selected SDOF system dimensions and boundary conditions are appropriate for the intended vibration characteristics. The ETABS model of the SDOF system is shown in Figure 3.

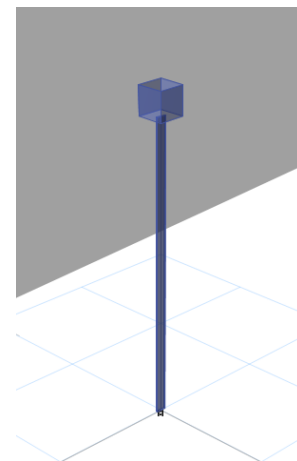


Figure 3: ETABS simulation of SDOF system for comparing time periods of B1 system.

#### 3.3. Experimental Observation and Displacement Response

Each SDOF system was physically fabricated based on the validated lengths. The maximum permissible displacement at the free end was calculated using the bending stress concept, ensuring that the SDOF system remained within the elastic limit during vibration. The SDOF system was then displaced to this permissible deflection and released, initiating free vibration. Permissible displacement calculation for each SDOF system is as shown in Table 3.

The displacement-time response was recorded using a Time-of-Flight (ToF) light reflection sensor, which accurately captured the vibration decay. A plot of displacement versus time of the SDOF system is presented in Figure 4.

#### 3.4. Determination of Damping Ratio

The recorded displacement-time data were processed in MATLAB to determine the damping ratio  $\xi$  of each SDOF system using the logarithmic decrement method. The analysis showed that the damping ratio exhibited only slight variations among the SDOF system. This indicates that, while minor experimental differences may affect the results, the overall damping behavior is primarily governed by the material properties, with energy dissipation largely determined by material damping. The damping ratios for each SDOF system, computed using MATLAB, are summarized in Table 4.

The damping ratios obtained in this study were compared against values reported in the literature to assess the validity of the experimental findings. Mevada and Patel (2016) experimentally determined the structural damping of metallic cantilever beams using LabVIEW and ANSYS.

Table 1: Length of cantilever beam calculated from different method

SDOF Designation	Target Time Period	Length from Lumped Mass Concept	Length from Finite Element Method	Length from Rayleigh Method
B1	0.50	0.6013	0.5877	0.5877
B2	0.75	0.7879	0.7651	0.7651
B3	1.00	0.9545	0.9215	0.9216
B4	1.25	1.1070	1.0639	1.0639

Table 2: Comparison of time periods for SDOF system: analytical calculations and ETABS results

SDOF System Designation	Target Time Period	Modelled Length in ETABS	Obtained Time Period	Percentage Difference
B1	0.50	0.6013	0.55	10%
B2	0.75	0.7879	0.818	5.053%
B3	1.00	0.9545	1.05	5%
B4	1.25	1.1070	1.362	11.44%

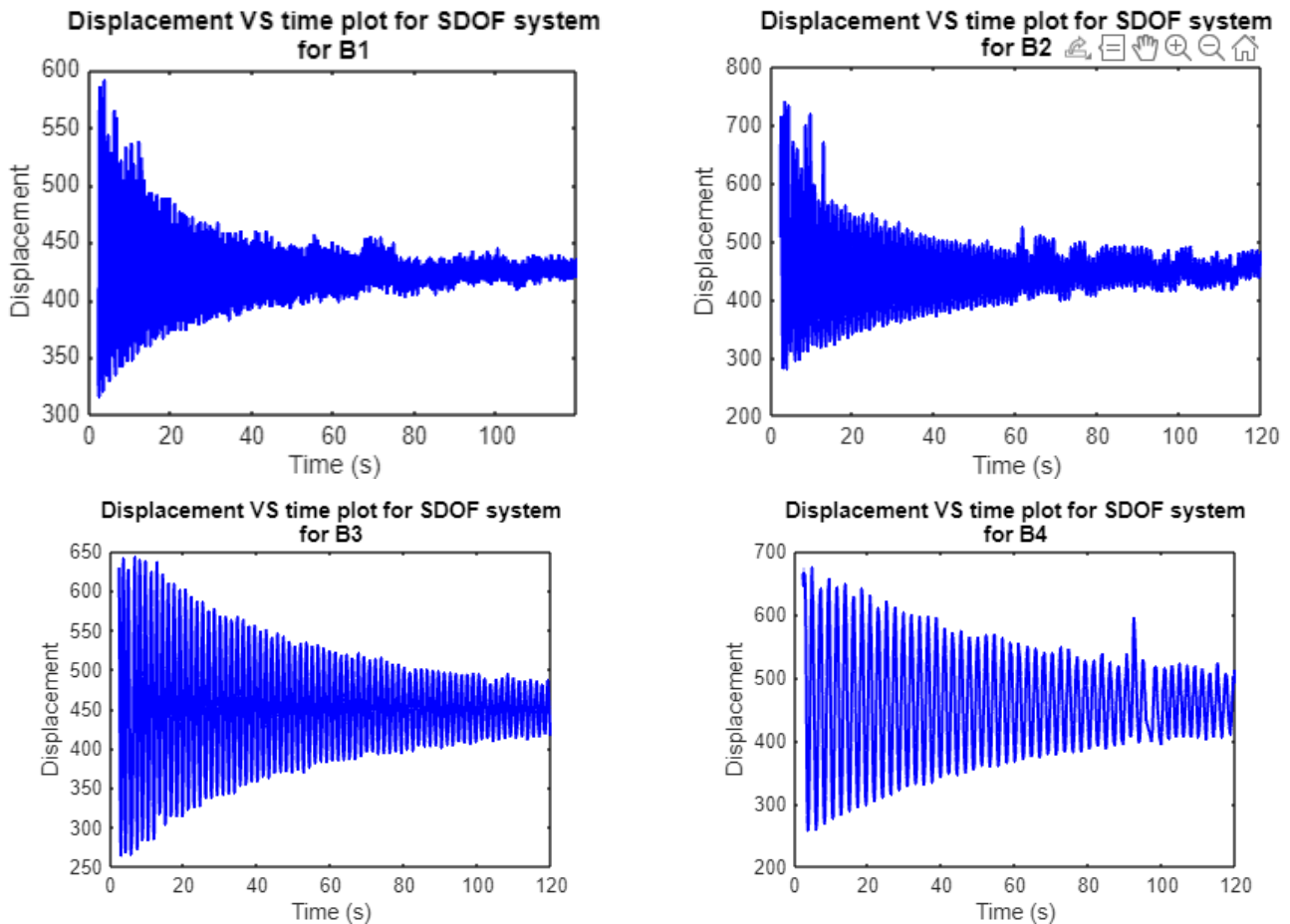


Figure 4: Displacement VS time plot of SDOF system B1, B2, B3, B4

Their study reported damping ratios of approximately 0.0069 for mild steel, with values for metallic materials typically lying in the range of 0.003–0.012.

In the present work, the damping ratios derived from the logarithmic decrement method for the four SDOF beam systems (B1–B4) ranged from 0.0042 to 0.0055.

Table 3: Permissible displacement at the top of the SDOF system

SDOF system Designation	SSDOF system length (mm)	(Permissible Displacement (mm))
B1	587.7	92.104
B2	765.10	156.10
B3	921.50	226.443
B4	1063.90	301.83

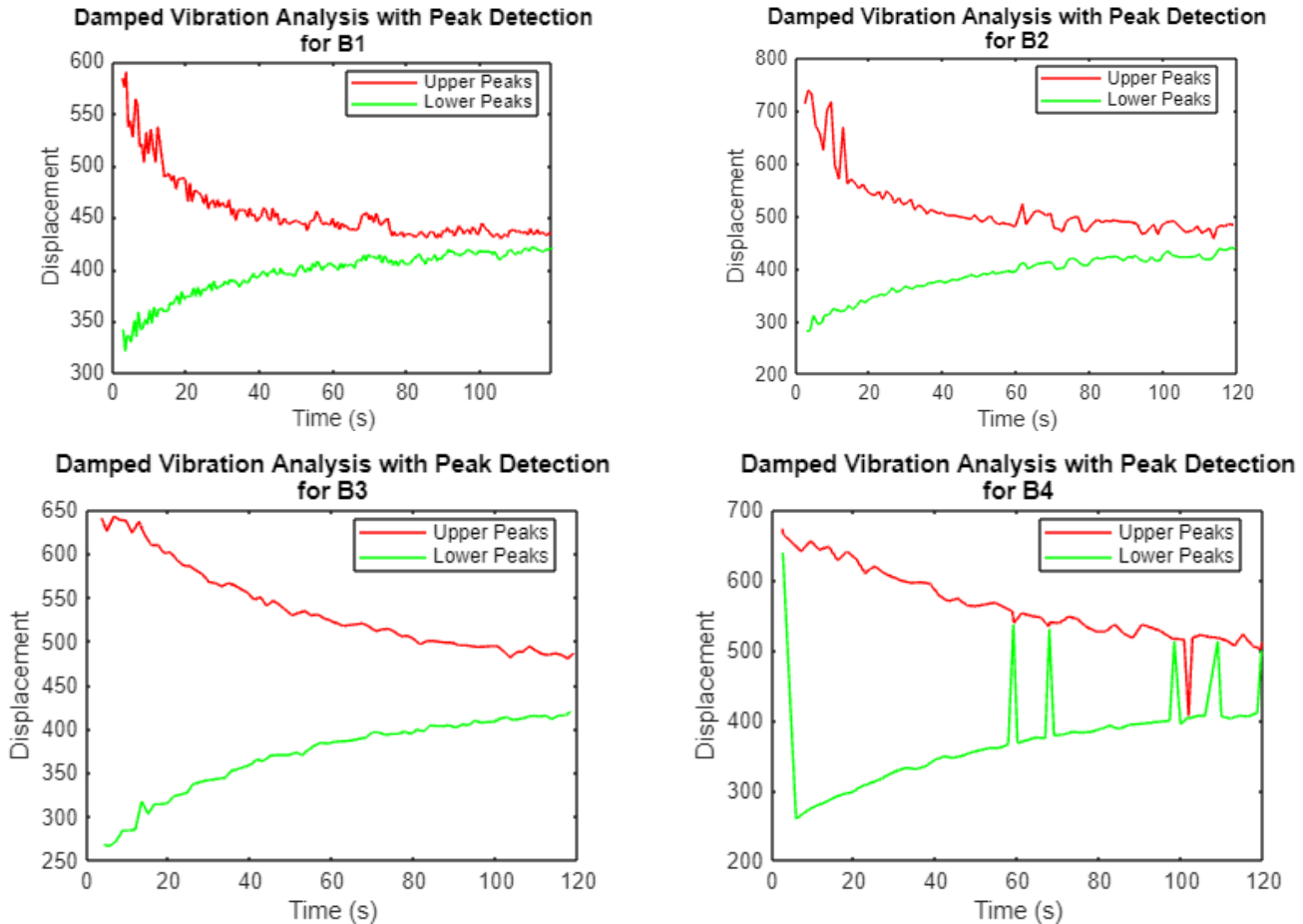


Figure 5: Peak displacement VS time plot of SDOF system B1, B2, B3, B4

These values show close agreement with the damping ratio range reported by Mevada and Patel (2016), confirming that the behaviour observed is characteristic of metallic beams dominated by material damping. Minor variations between the present results and those from literature are expected and may arise from differences in beam geometry, boundary conditions, surface condition, mass distribution, and measurement techniques.

Overall, the comparison demonstrates that the experimentally evaluated damping ratios in this study are consistent with those previously reported for steel cantilever beams. This agreement validates the adopted

experimental methodology and confirms that the damping behaviors is primarily governed by material damping mechanisms.

#### 4. Conclusion

This study determined the damping ratio ( $\xi$ ) of SDOF system using experimental free vibration tests and MATLAB-based data processing. The SDOF system were modeled in ETABS to validate the time periods corresponding to the designed SDOF system lengths, showing very good agreement between the target and

Table 4: Damping ratio values for the tested SDOF system B1-B4

SDOF System Designation	Target Time Period	Modelled length	Obtained Damping Ratio $\xi$ from Upper peak	Obtained Damping Ratio $\xi$ from lower peak	Overall Average Damping Ratio $\xi$
B1	0.50	0.6013	0.004099	0.004099	0.004202
B2	0.75	0.7879	0.004601	0.006334	0.005467
B3	1.00	0.9545	0.003569	0.005824	0.004696
B4	1.25	1.1070	0.004854	0.005540	0.005197

modeled values.

The experimentally obtained damping coefficients for each SDOF are summarized in Table 4. The results show slight variations among the SDOF system, with overall average damping coefficients ( $\xi$ ) ranging from 0.0042 to 0.0055. These variations are within expected experimental limits and indicate that the damping behaviour is primarily governed by material properties.

MATLAB proved to be an effective platform for processing displacement–time data and calculating damping ratios using the logarithmic decrement method, ensuring accuracy and reproducibility. Overall, the study establishes a reliable experimental framework for determining damping coefficients of SDOF system, which can be extended in future work to investigate effects such as temperature variation, different boundary conditions, and other dynamic parameters.

The main limitation of this work is related to the data acquisition system. The sensor used can record data only at a time interval of 100 ms, which may result in missing some vibration peaks and introduce minor errors in the calculated damping coefficients. Additionally, only a single set of data was recorded for each specimen; taking multiple datasets would help reduce experimental error. The study also did not focus on the influence of boundary conditions (e.g., fixed versus bolted support), which could affect the results. Despite these limitations, the experimental setup provides a reliable platform for determining damping coefficients and can be expanded in future studies to investigate effects such as varying temperatures. Furthermore, this arrangement can serve as a laboratory tool to demonstrate fundamental concepts of single degree of freedom (SDOF) systems, including natural time period, damping coefficients, and displacement–time plots.

## References

- Brahmam, K. G. (2022). Experimental studies on estimation of damping: Cantilever beam.
- Chopra, A. K. (2007). *Dynamics of structures: Theory and applications to earthquake engineering* (4th). Pearson.
- Clough, R. W., & Penzien, J. (1975). *Dynamics of structures*. McGraw-Hill.

Desai, N. V. (2021). Calculation of damping factor for steel plate with rubber coating and without rubber coating by using fast fourier transform and dewesoft software in forced vibration system. *International Research Journal of Modernization in Engineering Technology and Science (IRJMETS)*, 3(1).

Mevada, H., & Patel, D. (2016). Experimental determination of structural damping of different materials. *Procedia Engineering*, 144, 110–115.

This work is licensed under a Creative Commons “Attribution-NonCommercial-NoDerivatives 4.0 International” license.



*This page is intentionally left blank.*